

Particle Velocity Interpolation in Block-Centered Finite Difference Groundwater Flow Models

DANIEL J. GOODE

Water Resources Division, U.S. Geological Survey, Reston, Virginia

A block-centered, finite difference model of two-dimensional groundwater flow yields velocity values at the midpoints of interfaces between adjacent blocks. Method of characteristics, random walk and particle-tracking models of solute transport require velocities at arbitrary particle locations within the finite difference grid. Particle path lines and travel times are sensitive to the spatial interpolation scheme employed, particularly in heterogeneous aquifers. This paper briefly reviews linear and bilinear interpolation of velocity and introduces a new interpolation scheme. Linear interpolation of velocity is consistent with the numerical solution of the flow equation and preserves discontinuities in velocity caused by abrupt (blocky) changes in transmissivity or hydraulic conductivity. However, linear interpolation yields discontinuous and somewhat unrealistic velocities in homogeneous aquifers. Bilinear interpolation of velocity yields continuous and realistic velocities in homogeneous and smoothly heterogeneous aquifers but does not preserve discontinuities in velocity at abrupt transmissivity boundaries. The new scheme uses potentiometric head gradients and offers improved accuracy for nonuniform flow in heterogeneous aquifers with abrupt changes in transmissivity. The new scheme is equivalent to bilinear interpolation in homogeneous media and is equivalent to linear interpolation where gradients are uniform. Selecting the best interpolation scheme depends, in part, on the conceptualization of aquifer heterogeneity, that is, whether changes in transmissivity occur abruptly or smoothly.

INTRODUCTION

Finite difference and finite elements solutions of the advection-dispersion equation exhibit unrealistic oscillation (overshoot and undershoot) and numerical dispersion when dispersivity is small [Pinder and Gray, 1977; Grove, 1977]. To eliminate these problems, the method of characteristics has been applied using moving particles to simulate advection, whereas finite difference [e.g., Konikow and Bredehoeft, 1978] or finite element [e.g., Neuman and Sorek, 1982] approximations simulate dispersion. Random walk models [e.g., Prickett et al., 1981] also simulate advection with moving particles but simulate dispersion by a particle Brownian motion. These particle methods, or any particle-tracking scheme, require transport velocities at particle locations that do not correspond to locations where velocity is known from solution of the flow equation (using finite difference or finite element methods).

The particle position in the x direction and travel time are related by

$$\int \frac{dx}{V_x} = \int dt \quad (1)$$

where V_x is the component of velocity in the x direction [LT^{-1}]. The presentation throughout much of this paper is for only the x component; expressions for the orthogonal y component are analogous. Evaluation of (1) requires the particle velocity along its path, whereas the numerical solution of the flow problem yields velocity at particular locations, such as nodes or midpoints of block interfaces, depending on the formulation of the method. For steady state flow, velocity at a specific location is constant, but velocity is a function of position along a particle's path line.

This paper is not subject to U.S. copyright. Published in 1990 by the American Geophysical Union.

Paper number 89WR03379.

Particle path lines are equivalent to streamlines in steady state flow.

Different interpolation schemes to determine the particle velocity may result in significantly different velocities, path lines, and travel times [Nicholson et al., 1987], especially for coarse discretization of heterogeneous media. These differences may be particularly important when using particle-type models of transport to investigate the effects of spatial variability of hydraulic conductivity [e.g., Smith and Schwartz, 1980; Davis, 1986; El-Kadi, 1988] or to verify analytical stochastic representations of transport in random aquifers [e.g., Ababou, 1988]. For the latter the numerical model is considered the true representation, and its accuracy is critical. The differences among interpolation schemes is a function of model discretization; in the limit the velocity change between nodes or elements is so small that the differences vanish. However, computational limitations, in general or for the computer on hand, continue to result in the use of relatively coarse grids, especially for three-dimensional problems.

For block-centered, finite difference models of groundwater flow, linear interpolation [$V_x = f(x)$] in the direction of the velocity component of interest [Reddell and Sunada, 1970] is consistent with the assumptions of the flow model; however, this method yields a discontinuous velocity field in homogeneous media. Bilinear interpolation [$V_x = f(x, y)$] has been used for particle velocities in two-dimensional models of solute transport [Garder et al., 1964; Konikow and Bredehoeft, 1978; Schwartz and Crowe, 1980; Prickett et al., 1981]. This method generates a continuous velocity field and has been widely applied for simulation of homogeneous media. However, this technique does not preserve discontinuities in velocity present in heterogeneous media when interpolation is performed across transmissivity contrasts [Goode, 1987].

The smoothness expected in the velocity field is related to the conceptualization of the variability of aquifer properties.

Aquifers are not ideally homogeneous, but velocity fields vary smoothly if the hydraulic properties of the aquifer vary smoothly. Velocity discontinuities occur at sharp changes in hydraulic properties such as a fault or layer boundary. A general and realistic interpolation scheme should yield smoothly varying velocities where hydraulic properties vary smoothly (or not at all) and discontinuous velocities at boundaries between different media.

This paper briefly reviews linear and bilinear interpolation and presents a new interpolation scheme for block-centered, finite difference, groundwater flow models [e.g., Konikow and Bredehoeft, 1978; McDonald and Harbaugh, 1988]. For several example problems the new scheme is shown to offer improved resolution of smoothly varying flow fields while preserving discontinuities at sharp boundaries. The presentation is for two-dimensional models, but the scheme is easily extended to three dimensions. In most cases of field scale aquifer simulation, transmissivity is more highly variable than porosity or saturated thickness, hence this study emphasizes velocity interpolation in systems with variable transmissivity.

SOLUTION OF THE FLOW EQUATION

The steady state two-dimensional groundwater flow equation can be solved using a block-centered finite difference representation. In heterogeneous media using constant block size the governing equation is approximated by [after Trescott *et al.*, 1976]

$$\frac{1}{\Delta x} \left\{ \left[T_{xx(i+1/2,j)} \frac{(h_{i+1,j} - h_{i,j})}{\Delta x} \right] - \left[T_{xx(i-1/2,j)} \frac{(h_{i,j} - h_{i-1,j})}{\Delta x} \right] \right\} + \frac{1}{\Delta y} \left\{ \left[T_{yy(i,j+1/2)} \frac{(h_{i,j+1} - h_{i,j})}{\Delta y} \right] - \left[T_{yy(i,j-1/2)} \frac{(h_{i,j} - h_{i,j-1})}{\Delta y} \right] \right\} = 0 \quad (2)$$

where T_{xx} and T_{yy} are the transmissivities in the x and y directions, respectively [L^2T^{-1}], h is the potentiometric head [L], Δx and Δy are the block widths or node spacings in, respectively, the x and y directions [L], and subscripts i and j are indices for the column (x) and row (y), respectively, of the finite difference grid (Figure 1). The notation $i + 1/2$ refers to the location of the block interface between columns i and $i + 1$. If saturated thickness is uniform, or the y dimension is vertical (a cross-sectional model), the transmissivity terms in (2) can be replaced by hydraulic conductivity, K [LT^{-1}]. Assumptions implicit in (2) include that there are no internal sinks or sources and that the grid is oriented along principal axes of the transmissivity tensor. The aquifer may be heterogeneous and anisotropic.

Solution of (2) yields head values at the block centers (nodes), and the bracketed terms in (2) are the negative of the discharges per unit width across the block boundaries (Figure 1). Velocity at the block interfaces can be calculated from the discharge at the interface, for example,

$$V_{x(i+1/2,j)} = \frac{q_{x(i+1/2,j)}}{\epsilon b} = \frac{-1}{\epsilon b} T_{xx(i+1/2,j)} \frac{(h_{i+1,j} - h_{i,j})}{\Delta x} \quad (3)$$

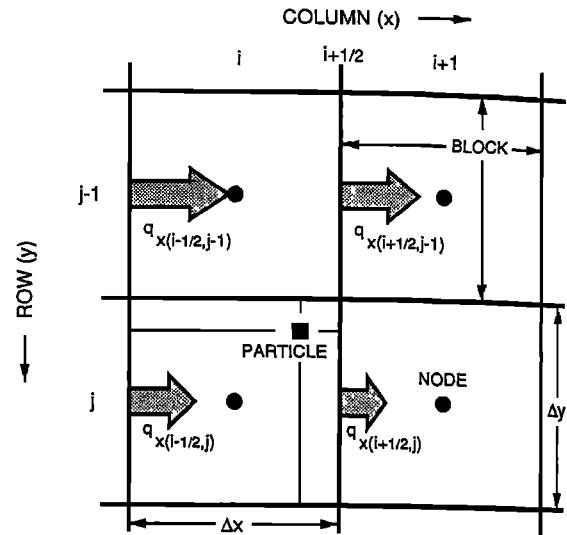


Fig. 1. Schematic of particle location and discharge components in the x direction in a block-centered finite difference grid.

where q_x is the discharge per unit width in the x direction [L^2T^{-1}], ϵ is the porosity [L^3L^{-3}], and b is the saturated thickness [L]. The velocity across each block face is determined by the head difference between the two adjacent nodes only. Porosity and saturated thickness may vary from block to block, and it is usually assumed that each is uniform within a block [Trescott *et al.*, 1976]. In this case the values of ϵ and b used in (3) depend on the block of interest, and V changes abruptly at the block interface.

The transmissivity terms in (2) and (3) represent the block interface values between adjacent blocks. This value is a function of the two block transmissivities, but the particular function chosen depends on the conceptualization of aquifer heterogeneity. A widely used function for determining the block interface transmissivity is the harmonic mean:

$$T_{xx(i+1/2,j)} = \frac{2T_{xx(i+1,j)}T_{xx(i,j)}}{T_{xx(i+1,j)} + T_{xx(i,j)}} \quad (4)$$

and similar expressions for the other terms in (2). This representation is exact for one-dimensional flow where the transmissivity is constant over each block and changes abruptly at block interfaces [Bear, 1979]. In natural systems, transmissivity may change abruptly at faults because of step changes in thickness. For cross-sectional models, hydraulic conductivity may change abruptly at layer boundaries. Equation (4) automatically yields a transmissivity value of zero if one of the blocks is impermeable.

The horizontal variability of model scale transmissivity in natural aquifers is often a smooth process because of gradual changes in thickness or lithology. If the specified transmissivity value is assumed to represent the point value at the node at the center of the block, and transmissivity is assumed to vary linearly between nodes, the exact block interface transmissivity value, for steady state one-dimensional flow, is [Appel, 1976]

$$T_{xx(i+1/2,j)} = \frac{T_{xx(i+1,j)} - T_{xx(i,j)}}{\ln \left(\frac{T_{xx(i+1,j)}}{T_{xx(i,j)}} \right)} \quad (5)$$

This value is larger than the harmonic mean but smaller than the arithmetic mean. This form cannot be used if the transmissivity is uniform or if one of the blocks has a zero value of transmissivity, but these cases can easily be handled separately. Another block interface value used is the geometric mean [Haverkamp et al., 1977], which is also the effective two-dimensional mean for an area within which transmissivity is lognormally distributed [Gutjahr et al., 1978]. Aquifer heterogeneity at a scale smaller than model blocks leads to macrodispersion [Gelhar and Axness, 1983]. In this work, however, the block values of transmissivity are considered effective block scale values, and the process of interest is the effect of large-scale variability, or trend, of block transmissivity on particle velocity. All of the numerical experiments use the harmonic mean for block interface transmissivity (4), except for the last case which uses the function of Appel [1976].

VELOCITY INTERPOLATION SCHEMES

Explicit linear displacements are typically used for particle movement: at a given time the particle's velocity is evaluated, and then this velocity is considered constant over a short time period and is multiplied by the time step size, yielding a displacement [x ≡ x₀ + Δt V_x(x = x₀, t = t₀)]. Changes in velocity during the step (curvature) are not incorporated, and particles do not follow streamlines for large time steps [Konikow and Bredehoeft, 1978]. Temporal integration along the path lines is an additional concern that is not addressed here. In this paper, explicit particle displacements are used, but time steps are sufficiently small so that particles essentially follow streamlines.

Linear Interpolation

Velocity at an arbitrary location within block (i, j) (Figure 1) can be computed by linear interpolation in the direction of the velocity component [Reddell and Sunada, 1970]:

$$V_x = (1 - f_x)V_{x(i-1/2,j)} + f_x V_{x(i+1/2,j)} \tag{6}$$

where

$$f_x = (x_p - x_{i-1/2})/\Delta x \tag{7}$$

An equivalent expression is

$$V_x = V_{x0} + \alpha(x_p - x_0) \tag{8}$$

where

$$\alpha = \frac{V_{xe} - V_{x0}}{x_e - x_0} \quad V_{x0} = V_x(t = t_0) \quad x_0 = x_p(t = t_0) \tag{9}$$

where x_p is the particle's x coordinate location, x₀ is the particle's location at time t₀, and subscript e refers to the exit block face: e = (i - 1/2, j) if V_{x0} < 0, and e = (i + 1/2, j) if V_{x0} > 0. Location x_e is the location of the exit block face, either x_{i+1/2} or x_{i-1/2}. Because the velocity varies linearly within a block, the exit boundary can be determined a priori from the starting velocity value when the particle enters the block. For the case of recharge within the block this scheme is consistent with the assumption of recharge distributed uniformly over the entire block. Within a block, V_x is a function of x only; changes in V_x in the y direction occur only at block interfaces, and V_x is not continuous across the top

and bottom block faces (the y faces) unless velocity is uniform. The expression relating particle position and travel time (1) can be integrated directly using (8) because V_x does not depend on y:

$$\frac{1}{\alpha} \left[\ln \left| \frac{V_{x0} + \alpha(x_1 - x_0)}{V_{x0}} \right| \right] = t_1 - t_0 \tag{10}$$

$$x_1 = x_0 + \frac{V_{x0}}{\alpha} \{ \exp [\alpha(t_1 - t_0)] - 1 \} \tag{11}$$

These expressions are undefined if V_x is uniform (α = 0), but then the position and time are simply related by x₁ = x₀ + V_x(t₁ - t₀). This method yields the exact location of the particle as it leaves each block with only one time step per block. However, smaller time steps must be used to illustrate the curved path line within a block.

Linear interpolation is consistent with the finite difference scheme used to solve the flow equation. The change in velocity within the block satisfies the governing flow equation:

$$\frac{\partial q_x}{\partial x} + \frac{\partial q_y}{\partial y} = 0 \tag{12}$$

where from (3) and (8)

$$\frac{\partial q_x}{\partial x} = \frac{\partial(\epsilon b V_x)}{\partial x} = \epsilon b \alpha \tag{13}$$

Substituting (9), with x₀ and x_e corresponding to the two faces, into (13), and substituting this expression and the analogous expression for the y components into (12) yields

$$\epsilon b \left[\frac{V_{x(i+1/2,j)} - V_{x(i-1/2,j)}}{x_{i+1/2} - x_{i-1/2}} + \frac{V_{y(i,j+1/2)} - V_{y(i,j-1/2)}}{y_{i+1/2} - y_{i-1/2}} \right] = 0 \tag{14}$$

This equation is equivalent to the finite difference equation (2) used to solve the governing flow equation, and hence the governing flow equation is continuously satisfied at all locations within the block. This consistency holds for any function used to determine block interface transmissivity.

Linear interpolation yields a discontinuous velocity field. The x velocity changes abruptly as a particle crosses a block boundary at y(j ± 1/2) and similarly for V_y at x(i ± 1/2).

Bilinear Interpolation

Bilinear interpolation of velocity incorporates linear changes in both directions for each velocity component [Garder et al., 1964; Konikow and Bredehoeft, 1978]:

$$V_x = (1 - F_y)[(1 - f_x)V_{x(i-1/2,j-1)} + f_x V_{x(i+1/2,j-1)}] + F_y[(1 - f_x)V_{x(i-1/2,j)} + f_x V_{x(i+1/2,j)}] \tag{15}$$

where

$$F_y = \frac{y - y_{j-1}}{\Delta y} \tag{16}$$

for the particle shown in Figure 1. In the case of variable porosity or thickness the velocity values from adjacent blocks in (15) are determined from fluxes using the porosity

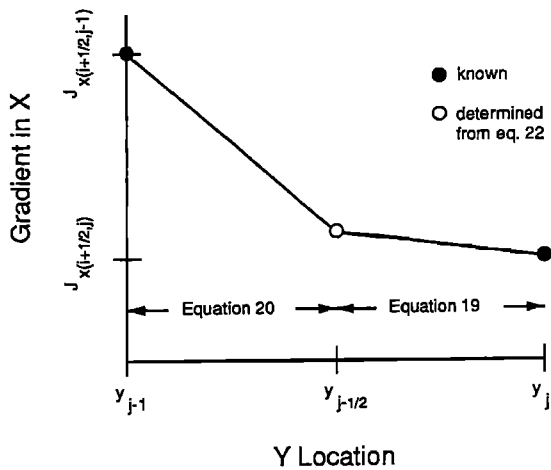


Fig. 2. Schematic of continuous interpolation of head gradient in the x direction ($J_x \equiv dh/dx$) as a function of y .

and thickness of the block where the particle of interest is located, for example,

$$V_{x(i+1/2,j-1)} = \frac{q_{x(i+1/2,j-1)}}{(\epsilon b)_{(i,j)}} \tag{17}$$

for the particle in Figure 1 located in block (i, j) . This method is analogous to a first-order Taylor series expansion in two dimensions. The particle position in (1) cannot be evaluated analytically for this method because V_x depends on the y location. Furthermore, this scheme does not result in a velocity field that necessarily satisfies the governing equation within each block. In particular, adjustments must be made near point sinks and sources [Konikow and Bredehoeft, 1978]. In general, the velocity field is continuous across block boundaries. Extensive experience with block-centered finite difference models using bilinear interpolation (particularly Konikow and Bredehoeft [1978] and Prickett et al. [1981]) indicate that it performs satisfactorily and does not introduce significant errors or inconsistencies. However, most model tests and applications have been for homogeneous media.

Grad Scheme

An alternate scheme (designated “grad” for brevity) can be developed that yields a continuous velocity field (for uniform porosity and thickness) except where transmissivity changes abruptly. The grad scheme uses bilinear interpolation of head gradients for each velocity component. The potentiometric head gradient in the direction parallel to a transmissivity zone boundary is continuous because head is continuous on the boundary. However, in the direction normal to the boundary the gradient changes abruptly because of conservation of discharge (refraction). A natural interpolation scheme, the grad scheme, can be developed assuming that head gradient in, for example, the x direction varies smoothly as a function of y and is continuous at y boundaries, $y = y(j \pm 1/2)$. The effective head gradients at the corners of blocks are determined such that interpolated fluxes preserve the net discharges of adjacent blocks. Bilinear interpolation of head gradients could be used to compute this corner value [Goode, 1987], but its multiplication with

the block interface transmissivities does not preserve the discharge from the finite difference solution of the flow equation.

At the center of a block face the x component of the effective head gradient, $J_x \equiv dh/dx [LL^{-1}]$, is, for example,

$$J_{x(i+1/2,j)} = \frac{(h_{i+1,j} - h_{i,j})}{\Delta x} \tag{18}$$

Note that physically the head gradient at this point is undefined if transmissivity changes at the boundary. However, this effective gradient is used because it yields the appropriate flux when multiplied by the block interface transmissivity. Assuming that the effective head gradient varies linearly in both directions within each block, and is continuous at block boundaries (Figure 2), the value of effective head gradient in the x direction on the block boundary at $x_{i+1/2}$ is, as a function of y ,

$$J_{x(i+1/2)}(y) = 2(1 - F_y)J_{x(i+1/2,j-1/2)} + [1 - 2(1 - F_y)]J_{x(i+1/2,j)} \tag{19}$$

for $y_{j-1/2} < y < y_j$ in block (i, j) and is

$$J_{x(i+1/2)}(y) = (1 - 2F_y)J_{x(i+1/2,j-1)} + 2F_yJ_{x(i+1/2,j-1/2)} \tag{20}$$

for $y_{j-1} < y < y_{j-1/2}$ in block $(i, j - 1)$. The head gradient at the block corner, $J_{x(i+1/2,j-1/2)}$, is as yet undefined. The discharge as a function of y in block (i, j) is (19) times the block interface transmissivity, which is constant for the block and is not a function of y . To preserve net discharge across the block face, the integral of discharge from y_{j-1} to y_j computed using (19) and (20) is set equal to one-half the sum of the discharges across the two block faces (from $y_{j-1/2}$ to $y_{j+1/2}$) from the finite difference equation:

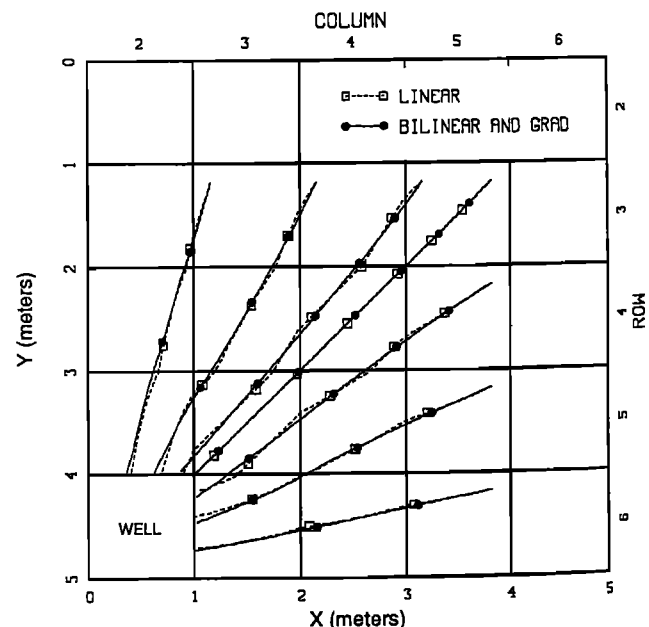


Fig. 3. Particle path lines for radial flow in a homogeneous aquifer (symbols are at equal time intervals).

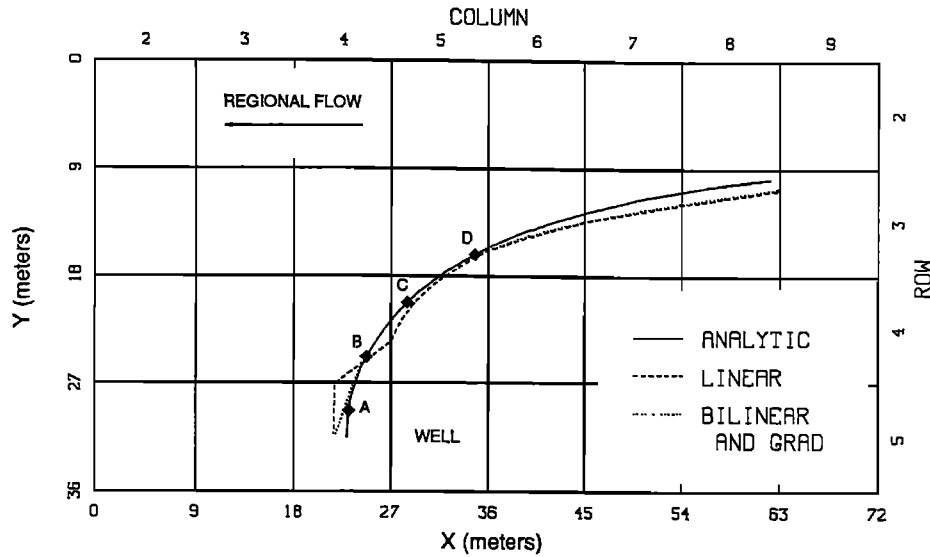


Fig. 4. Capture zone boundary for flow to a well in a uniform, regional flow field (computed velocities at labeled locations are shown in Table 1).

$$-T_{xx(i+1/2,j)} \int_{y_{j-1/2}}^{y_j} J_{x(i+1/2)}(y) dy - T_{xx(i+1/2,j-1)} + [1 - 2(1 - F_y)][(1 - f_x)V_{x(i-1/2,j)} + f_x V_{x(i+1/2,j)}] \quad (24)$$

$$\int_{y_{j-1}}^{y_{j-1/2}} J_{x(i+1/2)}(y) dy = \frac{\Delta y}{2} [q_{x(i+1/2,j)} + q_{x(i+1/2,j-1)}] \quad (21)$$

Substituting (19) and (20) into (21), evaluating the integrals, and solving for the corner head gradient at $(i + 1/2, j - 1/2)$ yields

$$J_{x(i+1/2,j-1/2)} = -\frac{q_{x(i+1/2,j)} + q_{x(i+1/2,j-1)}}{T_{xx(i+1/2,j)} + T_{xx(i+1/2,j-1)}} \quad (22)$$

To compute the velocity at the block corner, this term is multiplied by the interface transmissivity for the block within which the particle is located and divided by sb for the block of interest, yielding

$$V_{x(i+1/2,j-1/2)} = \frac{V_{x(i+1/2,j)} + V_{x(i+1/2,j-1)}}{T_{xx(i+1/2,j)} + T_{xx(i+1/2,j-1)}} T_{xx(i+1/2,j)} \quad (23)$$

for particles in block (i, j) . Again, if porosity or thickness are variable, the effective velocity from the adjacent block is the flux divided by sb for the block of interest (see (17)). Although the effective gradient is continuous at the point $(i + 1/2, j - 1/2)$, the velocity is discontinuous if the block interface transmissivities are not equal. Note that (23) reduces to an arithmetic average if transmissivity is uniform. For particles in block $(i, j - 1)$ the last transmissivity term in (23) would be changed to $T_{xx(i+1/2,j-1)}$ and the porosity and thickness of block $(i, j - 1)$ would be used to determine all V_x .

A bilinear interpolation scheme within block (i, j) for the x velocity of the particle shown in Figure 1 is then

$$V_x = 2(1 - F_y)[(1 - f_x)V_{x(i-1/2,j-1/2)} + f_x V_{x(i+1/2,j-1/2)}]$$

where $V_{x(i+1/2,j-1/2)}$ is given by (23) and

$$V_{x(i-1/2,j-1/2)} = \frac{V_{x(i-1/2,j)} + V_{x(i-1/2,j-1)}}{T_{xx(i-1/2,j)} + T_{xx(i-1/2,j-1)}} T_{xx(i-1/2,j)} \quad (25)$$

For homogeneous media this scheme is equivalent to bilinear interpolation of velocity. If head gradients in the x direction are not a function of y , this method is equivalent to linear interpolation in homogeneous and heterogenous media.

NUMERICAL EXPERIMENTS

The general characteristics of the three interpolation schemes described above can be illustrated by numerical experiments that incorporate typical features of groundwater flow fields. Furthermore, the relative accuracy of each scheme can be shown by comparison with analytical solutions, if available, or with numerical solutions with minimal

TABLE 1. Velocity at Selected Locations for a Pumped Well in Regional Flow

Location*	Velocity Component	Velocity, 10^{-5} m/s		
		Analytic	Linear Interpolation	Bilinear Interpolation
D	V_x	-6.19	-6.28	-6.61
	V_y	+2.99	+3.27	+2.80
C	V_x	-4.49	-4.13	-4.36
	V_y	+3.96	+4.79	+3.94
B	V_x	-2.02	-3.35	-2.14
	V_y	+3.54	+2.27	+3.49
A	V_x	-0.25	+0.68	-0.33
	V_y	+1.42	+1.14	+1.64

*Locations shown in Figure 4.

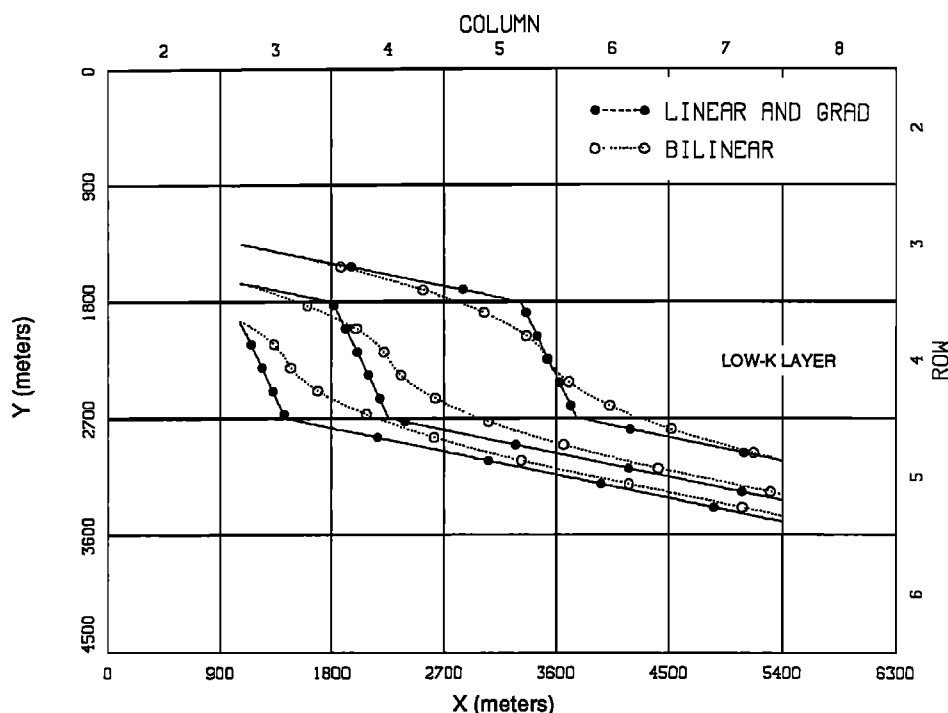


Fig. 5. Particle path lines for refractive flow across a low-hydraulic-conductivity layer (low K/high K = 0.1; symbols are at equal time intervals).

discretization error. The following cases are presented: radial flow in a homogeneous aquifer, flow to a well in a uniform, regional flow field, refractive flow across a low-hydraulic-conductivity layer, nonuniform flow across a low-hydraulic-conductivity layer, nonuniform flow in a block-heterogeneous aquifer, and nonuniform flow in a smoothly heterogeneous aquifer. These cases have nonuniform flow or variable hydraulic properties or both features together. Relatively coarse discretization is used to illustrate the differences among the interpolation schemes. For the first three cases, analytical solutions are available to evaluate the interpolation results. Analytical solutions are not available for the last three numerical experiments. To evaluate the accuracy of the interpolation schemes for these cases, results of each scheme using the coarse grid are compared to results using a much finer grid. The fine grid results presented use the linear interpolation scheme. Each of the interpolation schemes yields essentially the same path lines at this level of discretization because the change in velocity across each block is small for the fine grid.

The numerical experiments use the general solute transport model of Konikow and Bredehoeft [1978] with modifications for alternate interpolation schemes and the use of Appel's [1976] function for block interface transmissivity for the last case. All cases are for steady state flow with uniform aquifer thickness and porosity so that only spatial transmissivity variability is examined, and the underlying assumptions of the model are not altered. In the figures the symbols on the path lines represent particle locations at selected times with equal time intervals between symbols hence closely spaced symbols indicate low velocity. Additional particle locations between those shown are indicated by the plotted path line. The coarse grid blocks are indicated by the gridding on each figure or by the major tic marks on the axes.

Radial Flow in a Homogeneous Aquifer

The first numerical experiment illustrates the differences among the interpolation schemes for a simple problem with uniform properties but nonuniform flow. The boundary conditions for this case (Figure 3) are fixed flux at the top and right (calculated analytically), no flux along the left and bottom, and fixed head in the well block (2, 6). The differences between computed velocities for bilinear and linear interpolation are greatest at the block boundaries; the interpolated velocities are identical at the block center or node. As a particle moves through a block, the differences are somewhat offsetting, and the bulk movement of the particles is very similar using the two methods, even for this coarse discretization. The streamlines should be straight lines into the well, as computed using bilinear interpolation. Because transmissivity is uniform in this case, the grad scheme is identical to bilinear interpolation of velocities.

Flow to a Well in a Uniform, Regional Flow Field

A similar numerical experiment, but with regional flow, shows the ability of the interpolation schemes to track a capture zone boundary and predict the location of a stagnation point. This aquifer is also homogeneous, but path lines curve into the well because of the additional component of regional flow. In addition, velocities change more rapidly in space, particularly near the stagnation point. The location of the capture zone boundary, which separates groundwater that flows into the well from groundwater that bypasses the well, is given by [after Bear, 1979]

$$\frac{y - Y_w}{x - X_w} = \tan \left[\frac{-2\pi q_r (y - Y_w)}{Q_w} \right] \quad y > Y_w \quad (26a)$$

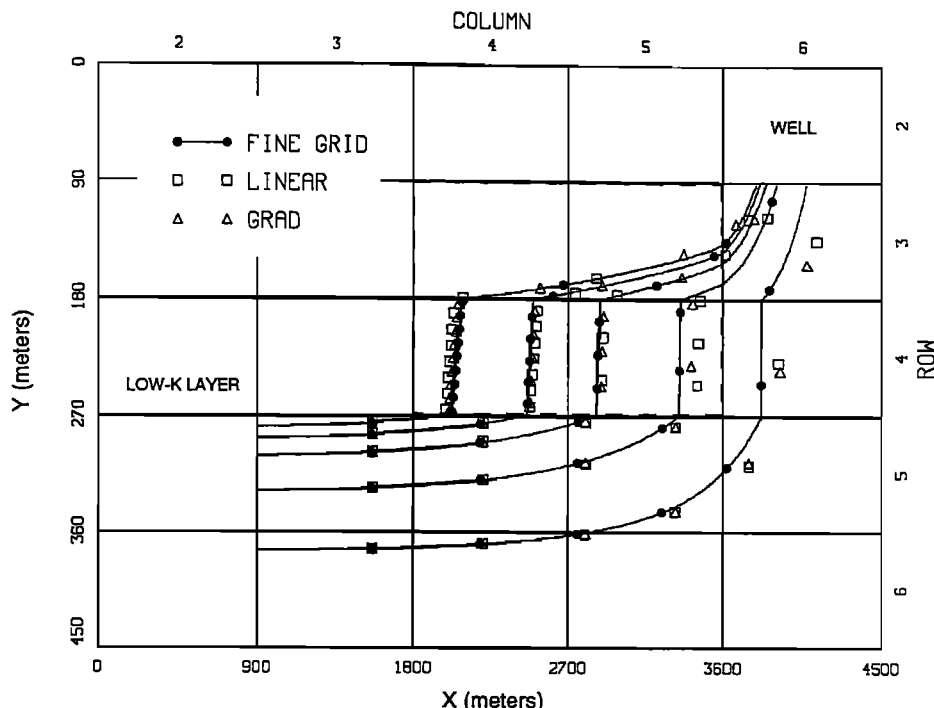


Fig. 6. Particle path lines for nonuniform flow across a low-hydraulic-conductivity layer (low K/high K = 0.01; symbols are at equal time intervals; dashed section enlarged in Figure 7).

$$\frac{y - Y_w}{x - X_w} = - \tan \left[\frac{-2\pi q_r (y - Y_w)}{Q_w} \right] \quad y < Y_w \quad (26b)$$

where q_r is the regional discharge per unit width in the x direction [L^2T^{-1}], Q_w is the well withdrawal rate [L^3T^{-1}], and the well is located at (X_w, Y_w) . The numerical model uses fixed heads on all boundaries (calculated analytically) and a fixed flux in the well block. The aquifer is simulated by eight columns and seven rows of active blocks, although only the upper four active rows are shown in Figure 4, as the problem is symmetric about $y = Y_w$. The well is centered at (31.5, 31.5), which is in block (5, 5). The capture zone boundary in the particle-tracking models is identified by two adjacent particle path lines, one of which enters the grid

block representing the well while the other bypasses the well and leaves the grid on the left boundary. The stagnation point is located between these two pathlines at $y = Y_w$.

Results for the case of a well pumping in a regional flow system are similar to the case of radial flow. Bilinear interpolation (that again is equivalent to the grad scheme because the aquifer is homogeneous) provides more accurate path lines near the well. Away from the well, the two interpolation schemes yield essentially identical path lines that are slightly removed from the analytical solution because of discretization errors in the flow solution. Velocities calculated at the labeled points in Figure 4 are presented in Table 1 for linear and bilinear interpolation and for the analytical solution. Bilinear interpolation yields more accurate velocities, particularly near the stagnation point. For location A, linear interpolation yields an x velocity in the wrong direction.

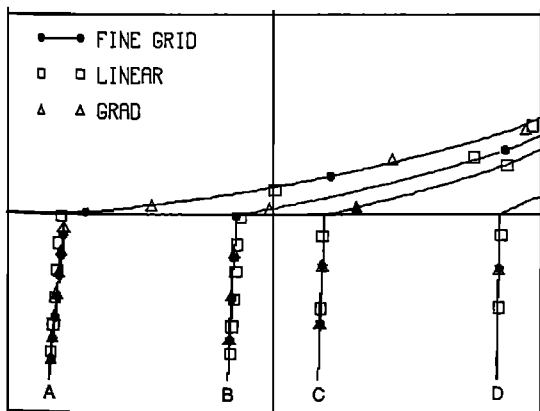


Fig. 7. Enlarged section of grid in Figure 6 showing path lines for particles initially released in the low-hydraulic-conductivity layer (computed velocities at labeled locations are shown in Table 2).

TABLE 2. Velocity at Selected Locations for Nonuniform Flow Across a Low-Hydraulic-Conductivity Layer

	Location*			
	A	B	C	D
	$V_x, 10^{-6} \text{ m/s}$			
Linear	1.50	1.50	1.49	1.49
Grad	1.42	1.36	1.31	1.15
Fine grid	1.42	1.37	1.31	1.17
	$V_y, 10^{-6} \text{ m/s}$			
Linear	2.68	2.68	7.11	7.11
Grad	2.09	4.16	5.63	10.86
Fine grid	1.86	3.31	5.18	9.07

*Locations shown in Figure 7.

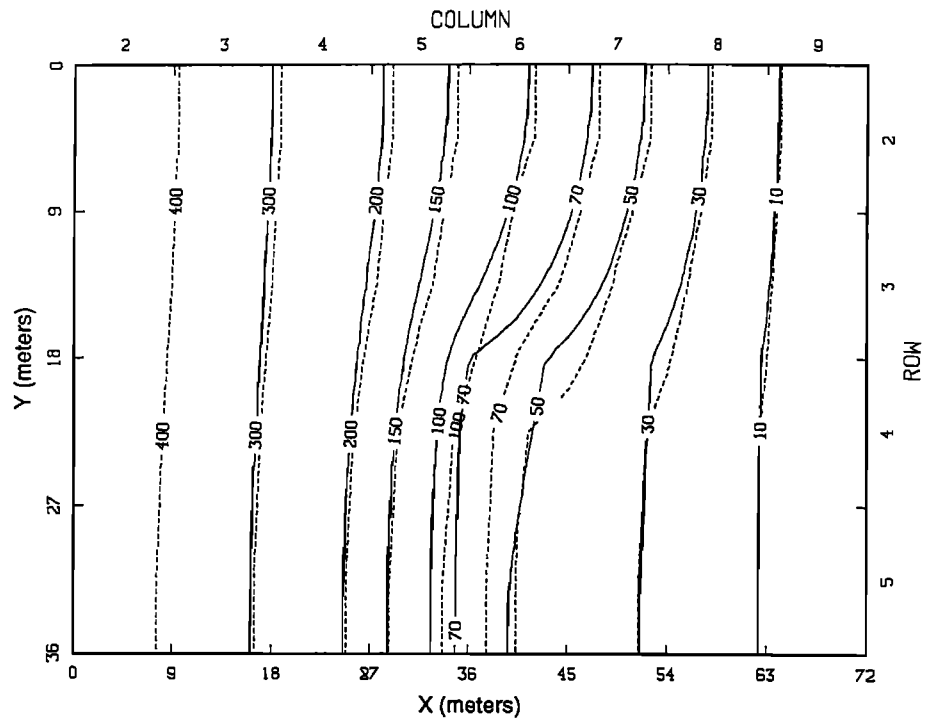


Fig. 8. Head contours for nonuniform flow in a block-heterogeneous aquifer (low K/high K = 0.1): fine grid (solid curves) and coarse grid (dashed curves).

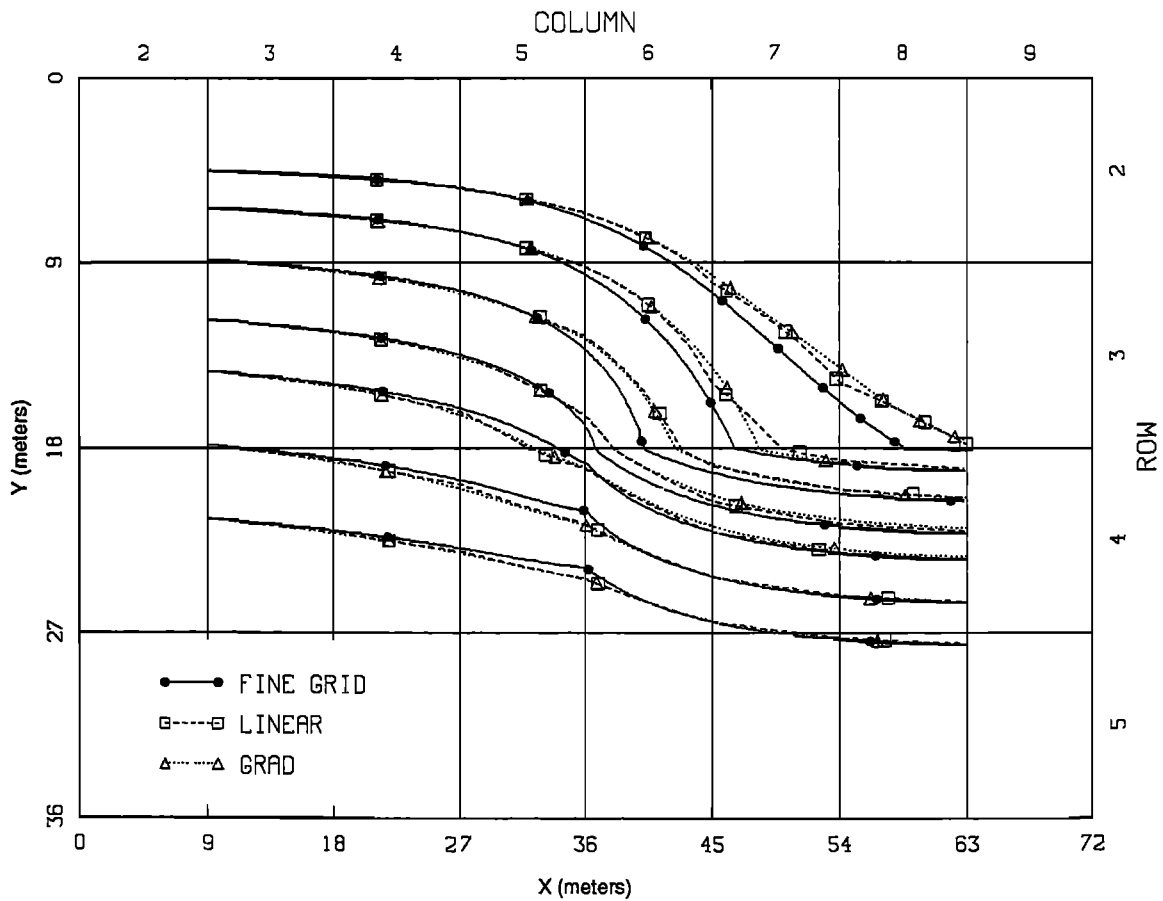


Fig. 9. Particle path lines for nonuniform flow in a block-heterogeneous aquifer (low K/high K = 0.1; symbols shown at equal time intervals).

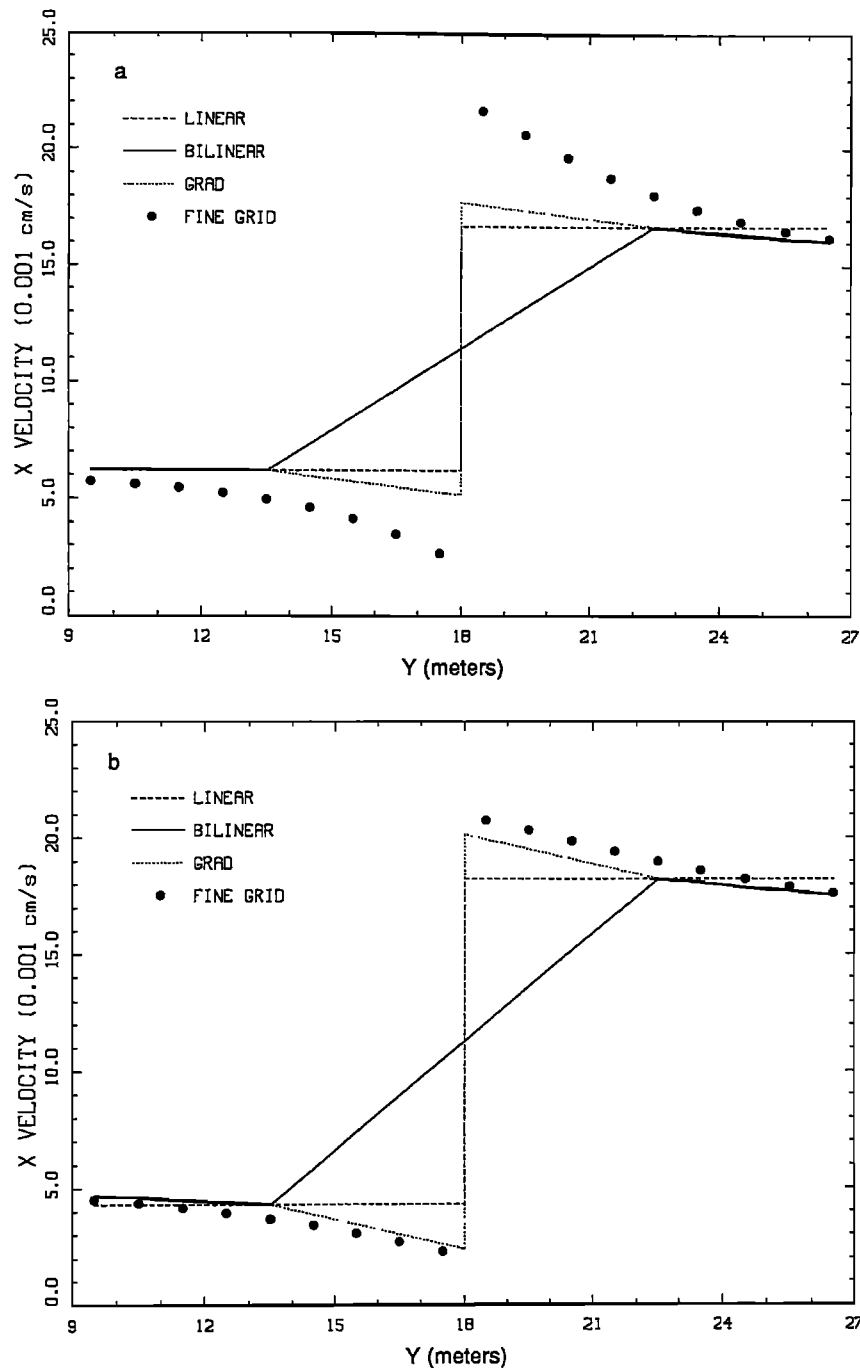


Fig. 10. V_x versus y for nonuniform flow in a block-heterogeneous aquifer: (a) at $x = 40.5$ m and (b) at $x = 44.5$ m.

Refractive Flow Across a Low-Hydraulic-Conductivity Layer

Streamlines are refracted at layer boundaries where hydraulic conductivity changes abruptly [Bear, 1979]. Figure 5 illustrates the grid used to simulate transport in a heterogeneous system in which flow crosses a layer having low-hydraulic-conductivity. The blocks in the middle row in Figure 5 have hydraulic conductivities one tenth of the values for the remaining blocks. Fixed heads on all boundaries are chosen to yield a uniform head gradient in the x direction and a uniform head gradient in the y direction except at the hydraulic conductivity boundary. Flux in the x

direction (parallel to the layering) is uniform within each layer, and flux in the y direction (normal to the layering) is uniform throughout the aquifer. Flow is from the upper left to the lower right.

Linear interpolation yields exact velocities for this example, showing the refraction effect, whereas bilinear interpolation of velocities smooths the x velocities and distorts the path lines (Figure 5). This smoothing occurs in the region within $1/2$ block width of the boundary on both sides. Path lines and velocities become more similar as the distance from the discontinuity increases because the error in particle position entering or approaching the heterogeneity is com-

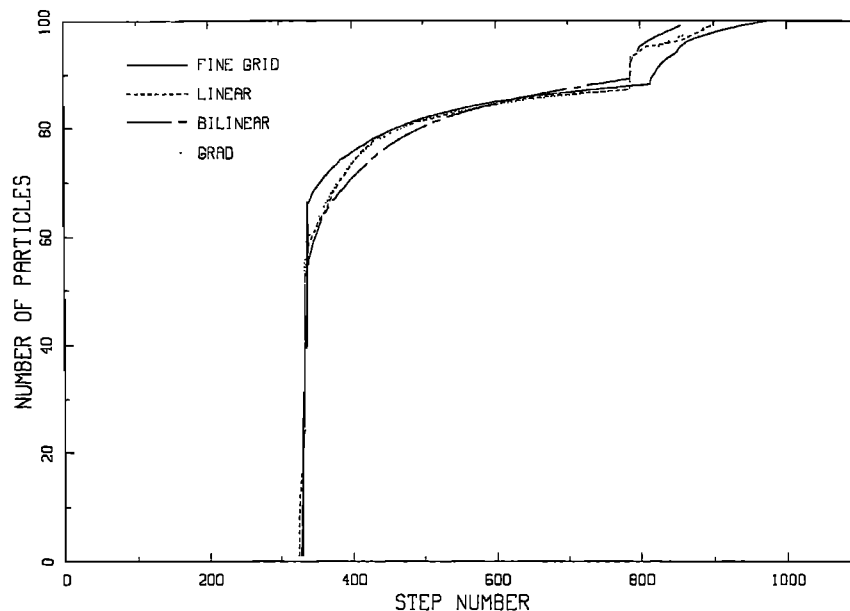


Fig. 11. Breakthrough of 100 particles for nonuniform flow in a block-heterogeneous aquifer.

compensated by an equivalent but opposite error when leaving the heterogeneity (note the top pathline in Figure 5). However, particles originating in the low-hydraulic-conductivity layer do not converge to the true path line using bilinear interpolation. For this case the head gradients in the x direction are not a function of y , and the head gradients in the y direction are not a function of x . Therefore the grad scheme is equivalent to linear interpolation of velocities and also yields, exactly, the refraction effect.

Nonuniform Flow Across a Low-Hydraulic-Conductivity Layer

Real aquifers are characterized by both nonuniform flow and variable hydraulic properties. Linear interpolation yields exact path lines for the preceding case because the velocity in the x direction is not a function of the y location within a block. The x velocity is constant within each block and changes abruptly at the boundary between the layers. In general, however, head gradients and velocities are not constant within each layer but change in response to boundary condition locations, strengths, and other factors. For these situations, velocity in the x direction may be a function of the x as well as the y coordinate location within a block. This numerical experiment of nonuniform flow across a low-hydraulic-conductivity layer has geologic characteristics similar to the preceding case but has variable velocity within each grid block. This case has a middle row of blocks in the coarse grid having one-hundredth the hydraulic conductivity of the remaining rows (Figure 6). As with typical cross-sectional models, Δx (horizontal) is larger (10 times) than Δy (vertical). Boundary conditions of fixed uniform head along the left boundary and withdrawal from the top right grid block of the coarse grid result in flow generally from left to right.

Because analytical solutions are not available for this and the following two cases, the results of the various interpolation schemes using a relatively coarse grid are evaluated by comparison to results from a much finer grid with $\Delta x(\text{fine}) =$

$\Delta x(\text{coarse})/9$, and $\Delta y(\text{fine}) = \Delta y(\text{coarse})/9$. Thus each block of the coarse grid corresponds to 81 blocks in the fine grid. This particular scaling (1/9) is used so that the node in the center grid block (of the 81) of the fine grid is located exactly at the location of a node of the coarse grid and equivalent boundary conditions can be imposed. The head solutions are different for the coarse grid and the fine grid because of different spatial discretizations. Although the linear interpolation scheme is directly consistent with the finite difference flow equation, the coarse grid provides a poorer approximation to the correct head field than the fine grid. The most accurate interpolation scheme is considered to be the one that yields velocities and path lines most closely agreeing with the fine grid results.

Results of the case of nonuniform flow across a low-hydraulic-conductivity layer indicate a difference between linear interpolation and the grad scheme that is not shown in the preceding case (refractive flow). Figure 6 shows particle positions for linear interpolation and the grad scheme on the coarse grid and the path lines for the fine grid. Results using bilinear interpolation of velocities (not shown) suffer from the same smoothing errors as previously shown for the refractive flow case. Figure 7 is an enlargement of four grid blocks showing the path lines of four particles released within the low-hydraulic-conductivity layer. The grad scheme more closely matches the fine grid results. For this example, V_y within the low-conductivity layer is a strong function of x because of the discharge location. However, for linear interpolation the change in V_y as a function of x only occurs at block boundaries; within a block, V_y is insensitive to x . Within one block, linear interpolation yields y velocities too high in the left half and too low in the right half (Table 2). The grad scheme partly incorporates the velocity variability exhibited in the fine grid results by allowing the y component of head gradient to vary in x . The grad scheme also preserves the discontinuity in V_x at the layer boundary by multiplying the interpolated gradient by the block interface transmissivity of the block where the particle is located (see Figure 7).

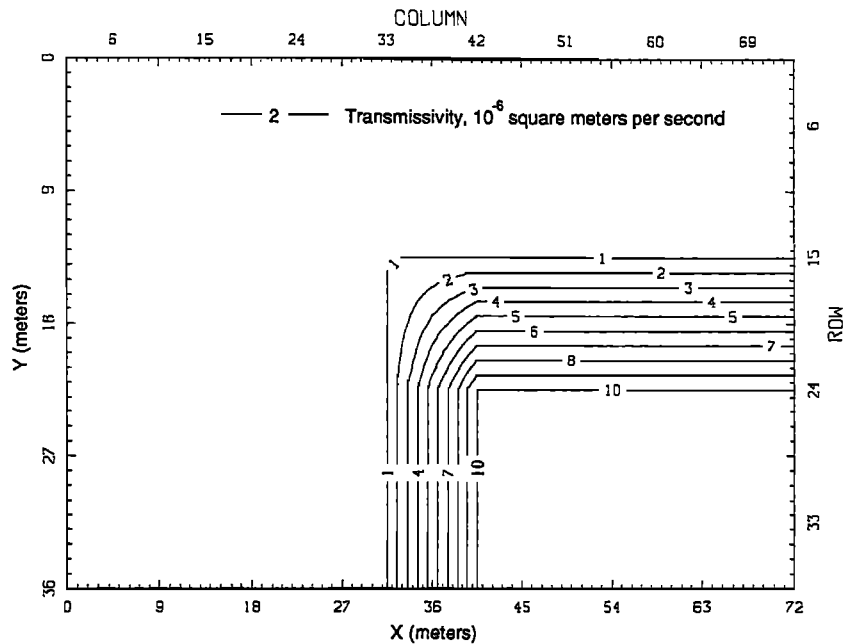


Fig. 12. Transmissivity contours for fine grid discretization of a smoothly heterogeneous aquifer.

Nonuniform Flow in a Block-Heterogeneous Aquifer

In addition to vertically layered systems, areal discontinuities in hydraulic properties may occur. Aquifer properties are often conceptualized as varying in a blocky fashion, perhaps because most available finite difference models assume that properties are uniform within a block. This numerical experiment shows interpolation scheme performance for systems having hydraulic discontinuities in both

directions, as opposed to layered systems. The lower right quadrant ($36 < x < 72$ m; $18 < y < 36$ m) of the aquifer shown in Figure 8 has a transmissivity 10 times higher than the remainder of the aquifer. Boundary conditions of fixed uniform flux into the aquifer on the left and fixed heads on the right yield the steady state heads shown in Figure 8 for the coarse grid and the fine grid. None of the interpolation schemes can completely account for the fact that the head solution using the coarse grid is not equivalent to the

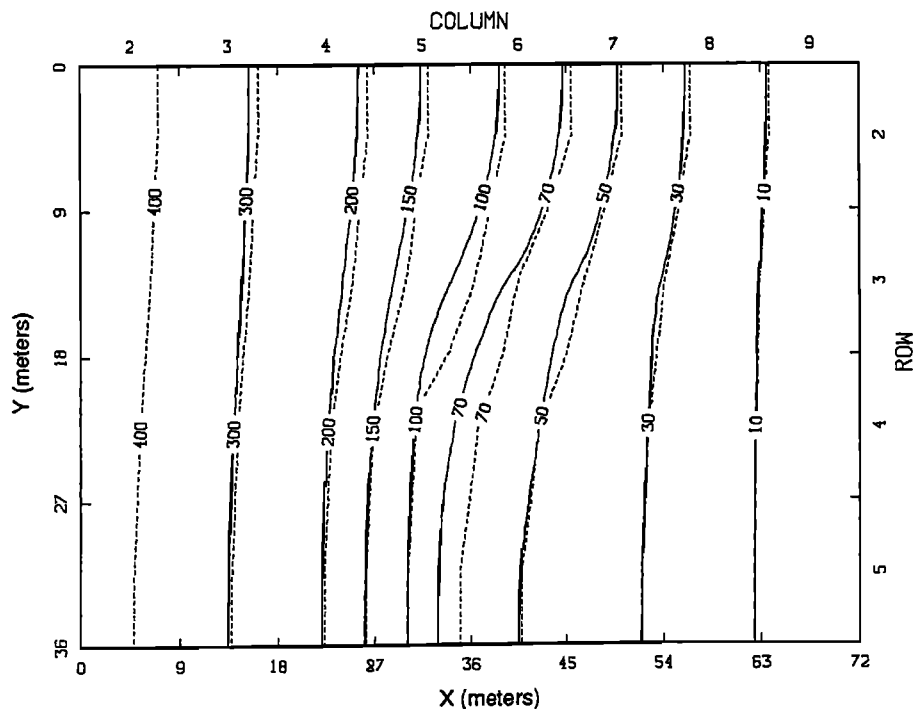


Fig. 13. Head contours for nonuniform flow in a smoothly heterogeneous aquifer: fine grid (solid curves) and coarse grid (dashed curves).

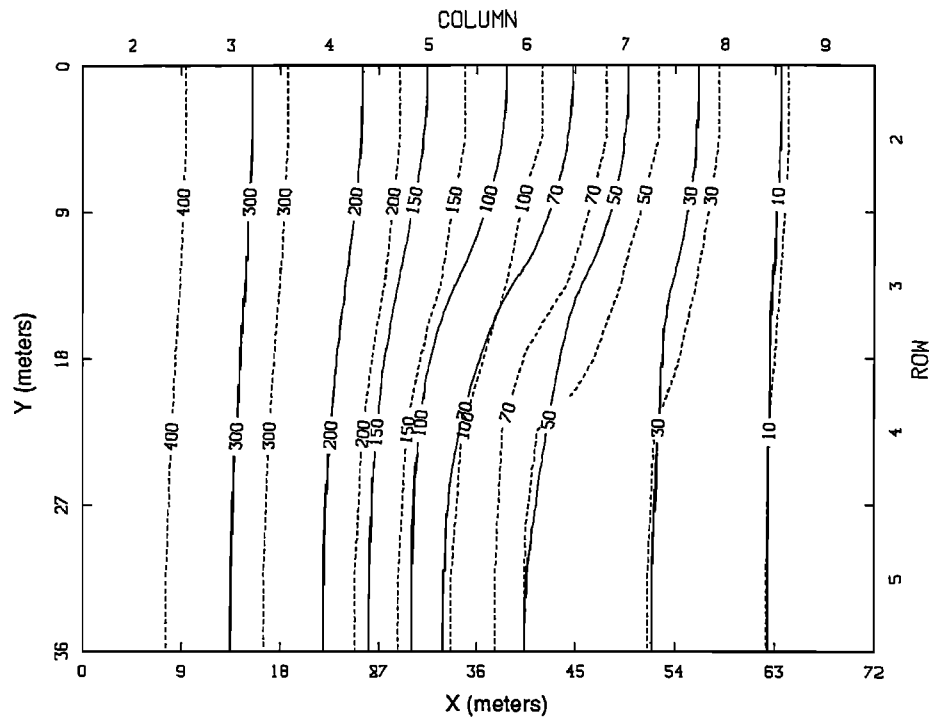


Fig. 14. Fine grid head contours (solid curves) for nonuniform flow in a smoothly heterogeneous aquifer compared to coarse grid solution using harmonic mean block interface transmissivity (dashed curves).

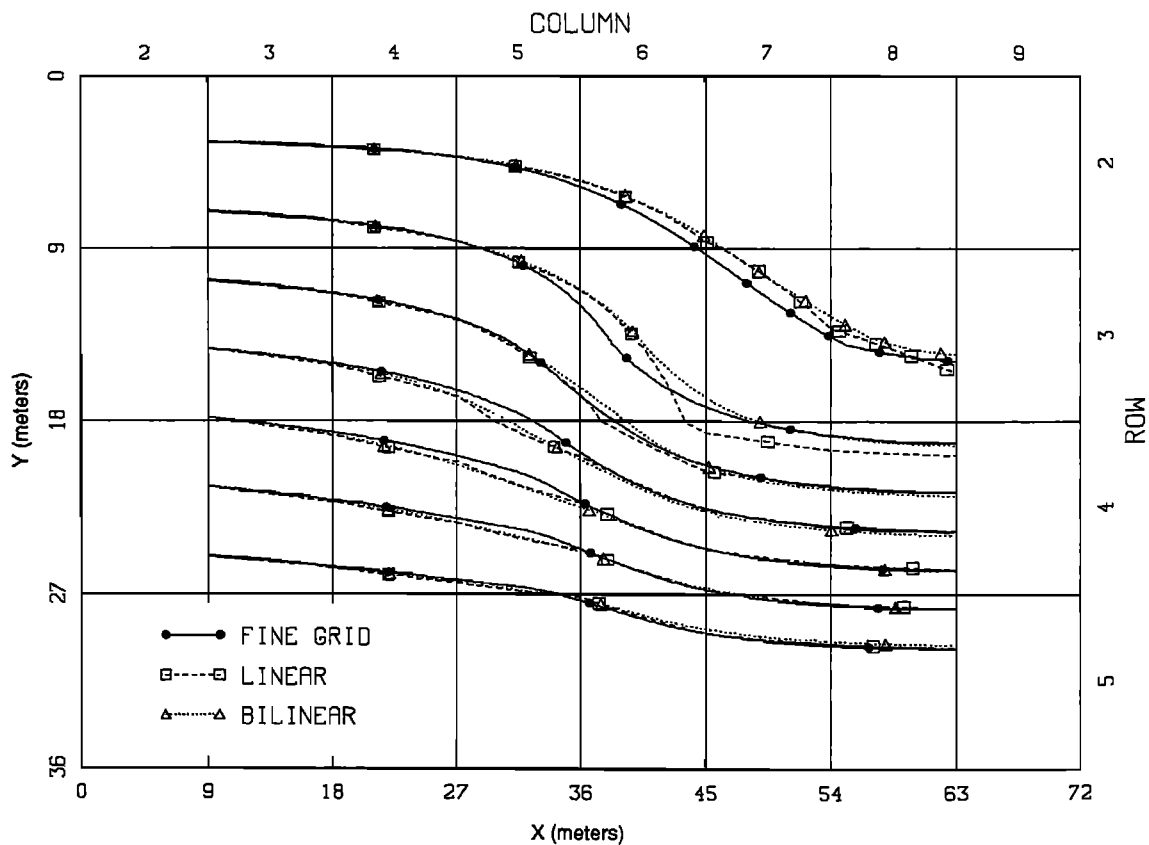


Fig. 15. Particle path lines for nonuniform flow in a smoothly heterogeneous aquifer (symbols are at equal time intervals).

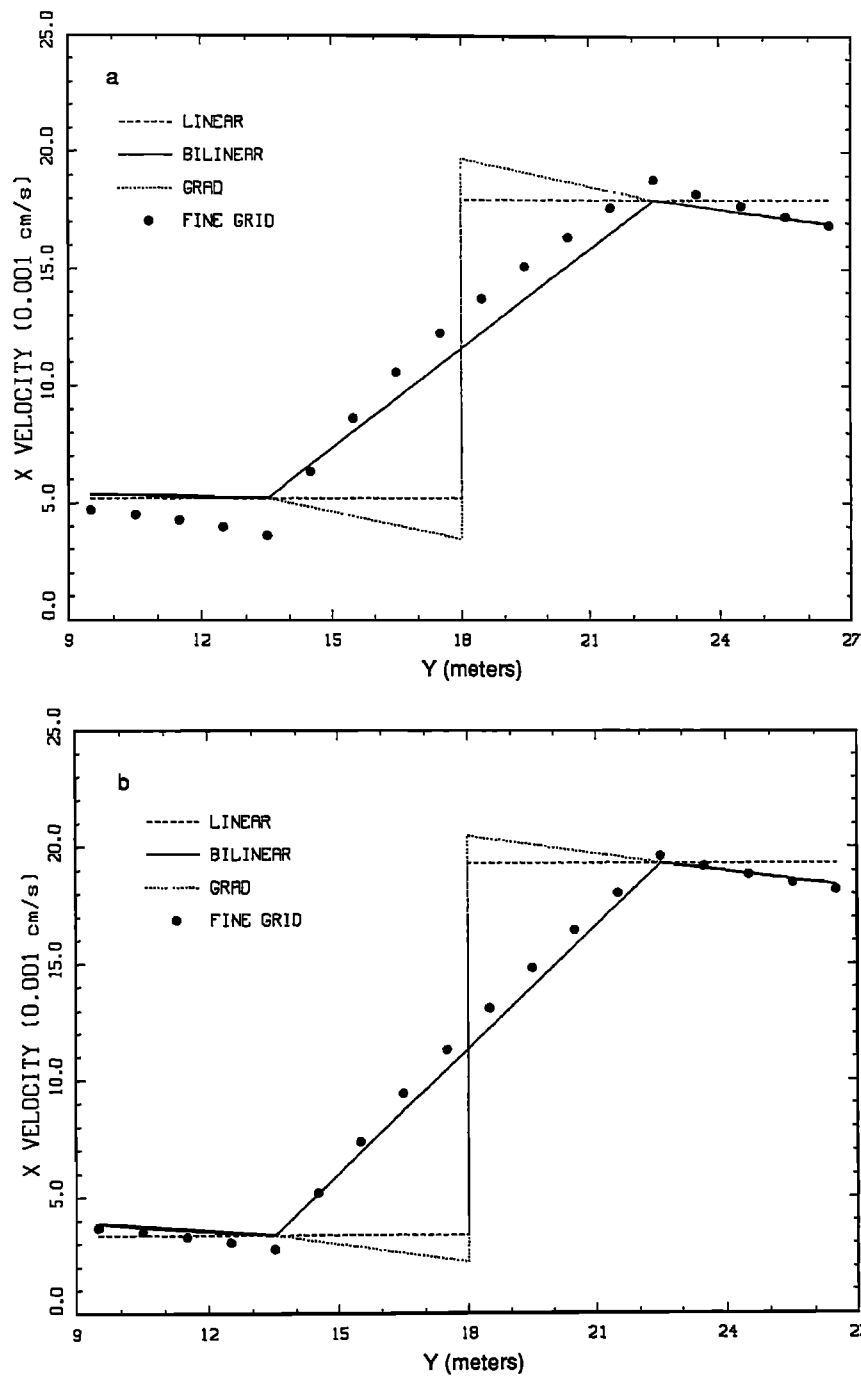


Fig. 16. V_x as a function of y for nonuniform flow in a smoothly heterogeneous aquifer: (a) at $x = 40.5$ m and (b) at $x = 44.5$ m.

solution obtained using the fine grid. The net discharges through the entire aquifer are identical because of the imposed boundary conditions. The y component of transmissivity is specified as zero in the first active column so that at $x = 9$ m V_x is uniform and V_y is essentially zero.

Results for the case of a block-heterogeneous aquifer using linear interpolation and the grad scheme are very similar for all path lines (Figure 9), but the path lines of the grad scheme appear more realistic near the transmissivity discontinuity. On most path lines the grad scheme yields a slightly better match than does linear interpolation for particle position at a given time (shown by symbols). Figure 10

shows V_x as a function of y for $9 < y < 27$ m: Figure 10a is for a vertical line at $x = 40.5$ m, Figure 10b is for a vertical line at $x = 44.5$ m. The lines extend from the y location of the boundary between rows 2 and 3 ($y = 9$ m) down to the boundary between rows 4 and 5 ($y = 27$ m). The velocity values shown for the fine grid are at the nodes of the fine grid and are identical for each of the interpolation schemes. As shown, the bilinear scheme smooths the abrupt change in V_x at the block boundary. For linear interpolation, V_x is constant over y within each block and changes abruptly at the block boundary. With the fine grid, however, V_x in the high transmissivity area increases toward the transmissivity

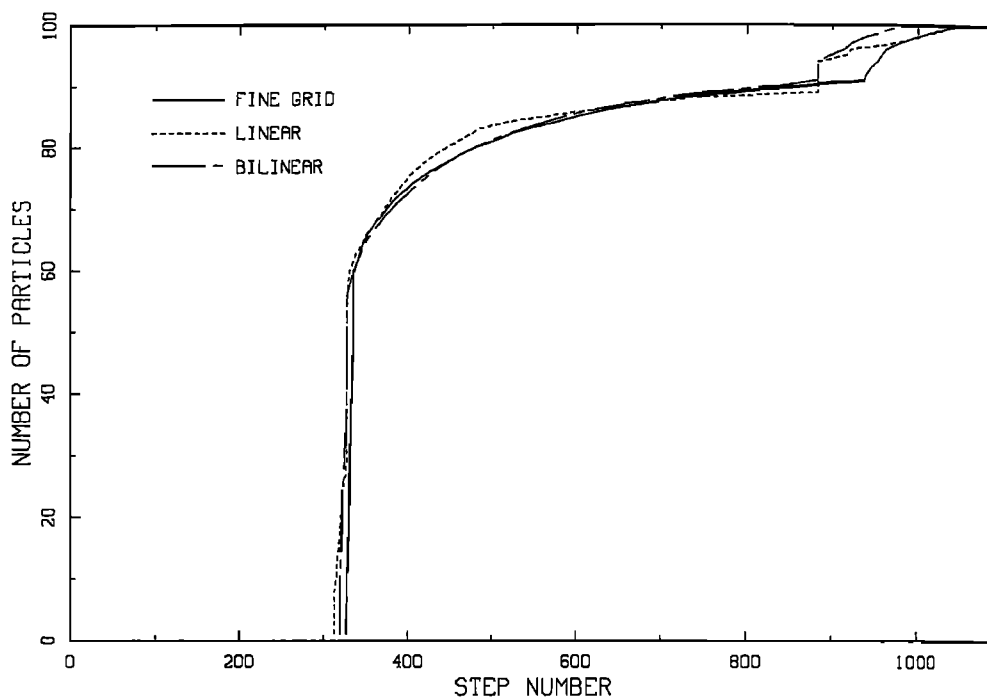


Fig. 17. Breakthrough of 100 particles for nonuniform flow in a smoothly heterogeneous aquifer.

boundary and in the low transmissivity area it decreases toward the boundary. At these locations the x direction gradient is higher in the low-transmissivity area and lower in the high-transmissivity area. By approximating the smooth variation in head gradient between the nodes of the coarse grid the grad scheme is able to partly account for this effect. All three of the interpolation schemes yield less variability in velocity than the fine grid solution.

A plot of breakthrough at the right boundary of 100 particles released in a vertical line at the left boundary also shows a reduction in travel time variability using the coarse grid solutions (Figure 11). All of the coarse grid schemes underestimate this variability and the spreading of the particles compared to the fine grid solution; the bilinear scheme is the poorest.

Nonuniform Flow in a Smoothly Heterogeneous Aquifer

Natural hydrogeologic systems may be conceptualized as having smooth rather than abrupt variability in hydraulic properties. If transmissivity is assumed to vary linearly between nodes of the finite-difference grid, then Appel's [1976] function (5) may be used for block interface transmissivity instead of the harmonic mean. Figure 12 shows the transmissivity field for this case, which is identical to the preceding case except for the smooth variability in transmissivity. For the coarse grid the block interface transmissivity at the discontinuity using the harmonic mean is 46% of the value using Appel's [1976] function. For comparison, the fine grid simulation explicitly incorporates the trend (see Figure 12) for the blocks located between the coarse grid nodes and uses Appel's function. At this scale the harmonic mean block interface transmissivity is at least 92% of Appel's function. Boundary conditions for this case are identical to the preceding case.

The coarse and fine grid heads for the case of smooth transmissivity (Figure 13) agree more closely than those in Figure 8 for the case of abrupt changes in transmissivity. The heads computed on the coarse grid using the harmonic mean transmissivity are a poor approximation to the results of the fine grid with smoothly varying transmissivity (Figure 14). The harmonic mean should not be used for block interface transmissivity if transmissivity is assumed to vary smoothly.

In contrast to the preceding case the smooth path lines generated using bilinear interpolation more closely match the fine grid results using a smooth transmissivity field than path lines using linear interpolation (Figure 15). The grad scheme (not shown) yields results similar to linear interpolation. Because the transmissivity changes smoothly, the linear and grad schemes do not represent the changes in velocity in the orthogonal direction accurately (Figure 16). For particle breakthroughs, bilinear interpolation best matches the fine grid results except for the slowest 10% of the particles (Figure 17). In contrast to the preceding example, the coarse grid results yield the first particles arriving before the first particles in the fine grid simulation.

DISCUSSION

Linear interpolation of velocities is directly consistent with the block-centered finite difference solution of the flow equation, and it is computationally attractive for particle tracking because in its integral form it is insensitive to time step size [Pollock, 1988]. However, this advantage is less significant if the curved path line within blocks is to be illustrated or if the particles are part of a general solute transport model with other time-stepping constraints, including transient flow. Linear interpolation produces a discontinuous velocity field, even for homogeneous media. Of course, the magnitude of this discontinuity depends on the discretization scale and may be acceptable for fine grids.

If transmissivity is considered uniform within each block, the grad scheme developed here is an improvement over linear interpolation for particle velocities. The grad scheme yields path lines that are similar to those from linear interpolation, but it more accurately accounts for velocity variability within blocks. Bilinear interpolation of velocity smooths the discontinuities in velocity that are consistent with the conceptualization of abrupt changes in hydraulic properties. When using bilinear interpolation to quantify dispersion in a block-heterogeneous aquifer [Davis, 1986; El-Kadi, 1988], dispersion is underestimated because velocity variability of the particles is less than the variability of the block interface velocity in the finite difference flow model. Furthermore, a coarse grid representation of the flow solution itself exhibits less velocity variability than the true system for the imposed heterogeneity. In recent numerical simulations of a two-dimensional block-heterogeneous aquifer, each transmissivity block had to be discretized by more than one finite difference grid block in order to reproduce global velocity variance (A. M. Shapiro, personal communication, 1988).

If transmissivity varies smoothly in space, Appel's [1976] function is more appropriate for determining block interface transmissivity and bilinear interpolation of velocity yields realistic path lines. For a given discretization, bilinear interpolation yields path lines more similar to finer grid results than linear interpolation, despite the fact that linear interpolation is directly consistent with the underlying numerical solution of the flow equation on the coarse grid.

Use of a finer grid in a heterogeneous system will yield a more accurate definition of the flow field near hydraulic conductivity and transmissivity contrasts and hence result in more accurate particle path lines. A finer grid will also minimize the model's sensitivity to the function used for determining block interface transmissivity and to the velocity interpolation scheme used. Simulations of nonuniform flow in heterogeneous aquifers using relatively coarse grids are most sensitive to these factors, and selection of the best methods requires care. In practical application the differences among these interpolation schemes may be minor compared to the errors in simulations induced by highly uncertain aquifer properties and boundary conditions. Nonetheless, for any given grid and problem definition it is desirable to use the most accurate interpolation scheme. For each time step, bilinear interpolation and the grad scheme require increased computation (two additional multiplications for each velocity component) compared to linear interpolation using explicit displacements. For many problems this increase will be small compared to the increase in computation for solving the flow problem and tracking more particles in a finer finite difference grid.

CONCLUSIONS

Selecting the best interpolation scheme to determine particle velocity in a groundwater flow model depends in part on the conceptualization of aquifer heterogeneity. Despite its inconsistency with the block-centered finite difference flow solution, the grad scheme developed here is more accurate than linear interpolation for particle velocities in block-heterogeneous systems. In the examples presented the inconsistency of the grad scheme on the block scale does not appear to introduce global error or divergence. If transmis-

sivity is assumed to vary smoothly, bilinear interpolation offers improved accuracy over both linear interpolation and the grad scheme. The additional computation of the grad scheme and bilinear interpolation (over that of linear interpolation) may be minor compared to increases from using a finer grid. Of course, a finer grid will always yield a more accurate definition of the flow field, particularly near discontinuities in hydraulic properties.

Acknowledgments. I am indebted to Leonard F. Konikow and Allen M. Shapiro for motivation, technical discussions, and support of this work. Suggestions by Richard W. Healy and Ward E. Sanford resulted in an improved manuscript.

REFERENCES

- Ababou, R., Three-dimensional flow in random porous media, 833 pp., Ph.D. thesis, Dep. of Civ. Eng., Mass. Inst. of Technol., Cambridge, 1988.
- Appel, C. A., A note on computing finite difference interblock transmissivities, *Water Resour. Res.*, 12(3), 561-563, 1976.
- Bear, J., *Hydraulics of Groundwater*, 569 pp., McGraw-Hill, New York, 1979.
- Davis, A. D., Deterministic modeling of dispersion in heterogeneous permeable media, *Ground Water*, 24(5), 609-615, 1986.
- El-Kadi, A. I., Remedial actions under variability of hydraulic conductivity, *J. Hydrol.*, 104, 327-344, 1988.
- Garder, A. O., Jr., D. W. Peaceman, and A. L. Pozzi, Jr., Numerical calculation of multidimensional miscible displacement by the method of characteristics, *Soc. Pet. Eng. J.*, 6(2), 175-182, 1964.
- Gelhar, L. W., and C. L. Axness, Three-dimensional stochastic analysis of macrodispersion in aquifers, *Water Resour. Res.*, 19(1), 161-180, 1983.
- Goode, D. J., Velocity interpolation schemes for advective transport in heterogeneous aquifers (abstract), *Eos Trans. AGU*, 68(44), 1290, 1987.
- Grove, D. B., The use of galerkin finite-element methods to solve mass-transport equations, *U.S. Geol. Surv. Water Resour. Invest. Rep.*, 77-49, 1977.
- Gutjahr, A. L., L. W. Gelhar, A. A. Bakr, and J. R. MacMillan, Stochastic analysis of spatial variability in subsurface flows, 2, Evaluation and application, *Water Resour. Res.*, 14(5), 953-959, 1978.
- Haverkamp, R., M. Vauclin, J. Touma, P. J. Wierenga, and G. Vachaud, A comparison of numerical simulation models for one-dimensional infiltration, *Soil Sci. Soc. Am. J.*, 41, 285-294, 1977.
- Konikow, L. F., and J. D. Bredehoeft, Computer model of two-dimensional solute transport and dispersion in ground water, 90 pp., *U.S. Geol. Surv. Tech. Water Resour. Invest. Book 7*, Chap. C2, 1978.
- MacDonald, M. G., and A. W. Harbaugh, A modular three-dimensional finite-difference ground-water flow model, 586 pp., *U.S. Geol. Surv. Tech. Water Resour. Invest. Book 6*, Chap. A1, 1988.
- Neuman, S. P., and S. Sorek, Eulerian-Lagrangian methods for advection-dispersion, in *Finite Elements in Water Resources, Proceedings of the 4th International Conference, Hannover, Germany, June 1982*, pp. 14.41-14.68, Springer-Verlag, New York, 1982.
- Nicholson, T. J., T. J. McCartin, P. A. Davis, and W. Beyeler, NRC experiences in Hydrocoin: An international project for studying ground-water flow modeling strategies, in *Proceedings of the Waste Management 87 Conference*, edited by R. G. Post, Univ. of Ariz., Tucson, 1987.
- Pinder, G. F., and W. G. Gray, *Finite Element Simulation in Surface and Subsurface Hydrology*, 295 pp., Academic, San Diego, Calif., 1977.
- Pollock, D. W., Semianalytical computational of path lines for finite-difference models, *Ground Water*, 26(6), 743-750, 1988.
- Prickett, T. A., T. G. Naymik, and C. G. Lonnquist, A "random-

- walk" solute transport model for selected groundwater quality evaluations, 103 pp., *Ill. State Water Surv. Bull.*, 65, 1981.
- Reddell, D. L., and D. K. Sunada, Numerical simulation of dispersion in groundwater aquifers, 79 pp., *Colo. State Univ. Hydrol. Pap.*, 41, 1970.
- Schwartz, F. W., and A. Crowe, A deterministic-probabilistic model for contaminant transport- Users manual, 158 pp., *Rep. NUREG/CR-1609*, U.S. Nucl. Regul. Comm., Washington, D. C., 1980.
- Smith, L., and F. W. Schwartz, Mass transport, 1, A stochastic analysis of macroscopic dispersion, *Water Resour. Res.*, 16(2), 303-313, 1980.
- Trescott, P. C., G. F. Pinder, and S. P. Larson, Finite-difference model for aquifer simulation in two dimensions with results of numerical experiments, 116 pp., *U.S. Geol. Surv. Tech. Water Resour. Invest. Book 7*, Chap. C1, 1976.
-
- D. J. Goode, U.S. Geological Survey, 431 National Center, Reston, VA 22092.

(Received April 11, 1989;
revised October 25, 1989;
accepted October 31, 1989.)